Ground-based millimeter and submillimeter-wave radiometry for the observation of the Arctic atmosphere

Domenico Cimini[1], Francesco Nasir[2], Fernando Consalvi[3] and Ed Westwater[4]

[1]CETEMPS, Università dell'Aquila, via Vetoio 1, 67100, L'Aquila, Italy
E-mail: nico.cimini@aquila.infn.it
[2]Osservatorio Astronomico di Cagliari, Cagliari, Italy
[3]Fondazione Ugo Bordoni, Roma, Italy
[4]Center for Environmental Technology, University of Colorado, Boulder, USA

Abstract

Microwave radiometers working at millimeter and submillimeter wavelengths show enhanced sensitivity to low contents of water vapor and cloud liquid in the atmosphere with respect to conventional radiometers working at centimeter wavelengths. This enhanced sensitivity gives particular interest to high-frequency radiometers for the accurate observations in extreme dry and cold conditions typical of the polar regions. Recent outcomes from modelling and experimental campaigns in the Arctic are hereafter presented and discussed, to demonstrate the feasibility and the accuracy of millimeter and submillimeter radiometric observations for the ground-based retrieval of thermodynamical properties of the atmosphere over polar regions.
Keywords: Atmosphere, Arctic, Microwave Radiometry.

Radiometria ad onde millimetriche e submillimetriche da terra per l'osservazione dell'atmosfera in artico

Riassunto

Radiometri a microonde operanti a lunghezze d'onda millimetriche e submillimetriche mostrano una sensibilità accentuata a contenuti bassi di vapore acqueo e acqua liquida in atmosfera rispetto ai radiometri convenzionali operanti a lunghezze d'onda centimetriche. Tale accentuata sensibilità conferisce ai radiometri ad alta frequenza un interesse particolare per osservazioni accurate nelle condizioni estremamente fredde e secche tipiche dei poli. In questo articolo vengono presentati e discussi i risultati di simulazioni e campagne di osservazione in Artico, che dimostrano la fattibilità e l'accuratezza di misure radiometriche ad onde millimetriche e submillimetriche da terra per stime di variabili termodinamiche dell'atmosfera ai poli.
Parole chiave: *Atmosfera, artico, radiometria a microonde.*

Introduction

The study of the polar atmosphere is extremely important for understanding the climate of our planet. In fact, water vapor and clouds in the Arctic play a key role in controlling the

Earth's climate, through greenhouse effect and the feedback on global ice coverage and sea surface temperature. Therefore, accurate measurements of the atmospheric water vapor and cloud properties in the Arctic are essential for improvement in modelling the energy budget of the Earth system.

Although the polar regions are frequently covered by satellite overpasses, the temporal and spatial resolutions provided by satellite-based remote sensing are rather coarse for microphysical studies. On the other hand, ground-based remote sensors provide continuous and accurate monitoring of the atmosphere microphysics on a local scale. In spite of this need, there is a lack of continuous measurements in the polar region due to the extreme and remote conditions, leading to large uncertainty in the radiative properties of the Arctic atmosphere. In addition, the lack of sensitivity of conventional instruments to low amounts of water vapor and cloud liquid makes it difficult to perform their measurements over the Arctic [Racette et al., 2005]. In fact, the Arctic region is characterized by extremely dry conditions; during winter, precipitable water vapor (PWV) and liquid water path (LWP) are usually below 5 mm and 0.2 mm [Shupe et al., 2005], respectively. For example, the occurrence and Cumulative Distribution Function (CDF) for PWV in Arctic winter conditions are shown in Figure 1, as extracted from a 6-year dataset of balloon-borne in situ radiosonde observations (RAOB).
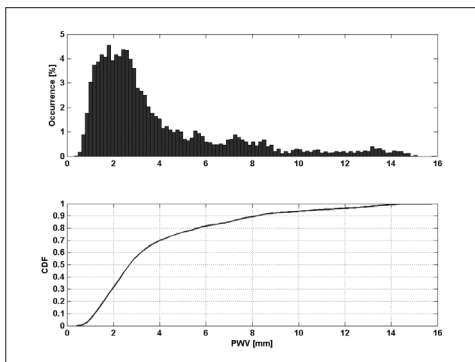

Figure 1 – Occurrence and Cumulative Distribution Function (CDF) for PWV in Arctic winter conditions as extracted from a 6-year dataset of RAOBs.
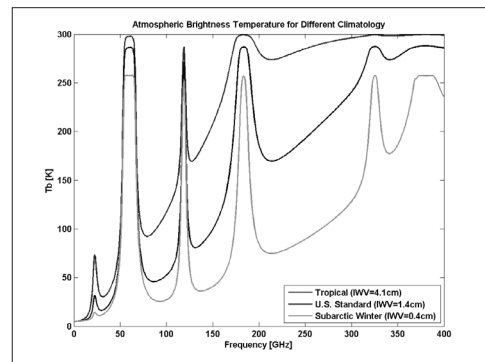

Figure 2 – Atmospheric downwelling brightness temperature for Tropical, U.S. Standard, and Arctic winter conditions.

Thus, the accuracy of existing instrumentation is limiting the development of theory and modelling of the radiative process in the polar atmosphere. As illustrated in Figure 2, the atmospheric opacity in the 1-400 GHz range shows an increase with frequency, due to absorption of the water vapor continuum, and peaks due to resonant absorption lines of oxygen (50-60, 118.75, and 368.49 GHz) and water vapor (22.235, 183.31, 325.15, and 380.20 GHz). In particular, the absorption at 183.31 and 380.20 GHz lines is 1 to 3 orders of magnitude larger than at 22.235 GHz. As the PWV increases, millimeter (mm) and submillimeter (submm) wavelengths (60-400 GHz) show significantly larger variations

with respect to centimeter (cm) wavelengths (10-30 GHz). Additionally, liquid water clouds contributes with absorption that roughly goes with the square of frequency (not shown), which causes the opacity due to liquid clouds to be larger for mm and submm channels than for lower frequency channels. These features translate into enhanced sensitivity of mm and submm wave to low amounts of PWV and LWP, which makes them appealing for deployment in very dry environments. Note that in moderate to humid environments (as in the Tropics), most mm and submm channels would gradually saturate (depending on PWV and frequency), and thus become more sensitive to temperature than humidity. Thus, the enhanced sensitivity of mm and submm radiometry comes at the expense of a higher degree of non-linearity with respect to conventional frequencies (20-30 GHz).

For the above reasons, few ground-based microwave radiometers were recently developed an tested, providing features that are very appealing for atmospheric research in very dry and cold environments, such as the poles and high-altitude regions.

In this paper, we illustrate the results obtained from data collected during two Arctic experimental campaigns, both involving a 28-channel radiometer called the Ground-based Scanning Radiometer (GSR).

Experimental Set-up

The GSR is a 28-channel radiometer recently developed at the Center for the Environmental Technology (CET) of the University of Colorado at Boulder (Colorado, USA). The set of GSR microwave channels was designed for the simultaneous retrieval of atmospheric temperature profile, water vapor content, cloud liquid path, and cloud depolarization ratio. In particular, referring to the spectrum of downwelling brightness temperature (Tb) in Figure 2:

- the 50-56 GHz channels are located in the strong oxygen absorption band and allow for atmospheric temperature estimates;
- the 183 and 380 GHz channels are located on the sides of two strong water vapor absorption lines (corresponding to different opacity depending upon distance from the line center) and allow for accurate observations of low water vapor contents;
- the horizontal (H) and vertical (V) polarization channels at 89 and 340 GHz are located in fairly transparent atmospheric regions (windows) and thus allow the study of cloud properties through the measurement of the emission and depolarization ratio;
- the remaining radiometer operates as an infrared broadband channel, measuring infrared brightness temperature (Tir) at 10.6 micron.

The GSR is calibrated using a combination of the three methods: internal reference loads, external targets, and tipping curve. The radiometric sensitivity at 1 s integration time for GSR microwave channels was measured in the laboratory, before the experiment, at room temperature and range from 0.05 to 0.2 K, depending upon channels. More details on the GSR design, calibration, and settings are given in [Cimini et al., 2007a].

Field Experiments

The first deployment of the GSR occurred during the Arctic Winter Radiometric Experiment (AWRE) [Westwater et al., 2004], held from March 9 to April 9 2004 at the U.S. Department of Energy Atmospheric Radiation Measurement (ARM) Program's North Slope of Alaska

(NSA) site in Barrow, Alaska (71° N, 156° W).

The major goal was to demonstrate that millimeter-wave radiometers can substantially improve observations of low vapor and liquid water. The ultimate purpose of the GSR deployment was to measure temperature, water vapor, and cloud properties, at cold (-20 to -55 °C) and dry (IWV < 5 mm) conditions. The GSR joined the ARM NSA resident microwave radiometer (MWR) and the microwave radiometer profiler (MWRP), operating at 22-58 GHz. Figure 3 shows a picture of the experimental set-up; about one month of observations were collected. More recently, the GSR was deployed during the Radiative Heating in Underexplored Bands Campaign (RHUBC), which was held in February - March 2007, again at the ARM NSA site. The conditions experienced during RHUBC can be expressed as follows: surface temperature ranging from -38 to -19 °C and PWV from 0.9 to 3.6 mm. The aim of RHUBC was to study radiative heating occurring in the far-infrared spectrum using accurate estimates of the water vapor content from independent and reliable sensors. Other than GSR, MWR, and MWRP, two other mm-wave radiometers were deployed, the Microwave Profiler MP-183A and the G-band water Vapor Radiometer (GVR). The GSR, GVR, and MP-183A all have several channels located around the strong 183.31 GHz water vapor line.

From the ARM NSA site, operational radiosondes are routinely launched once to twice a day. These operational radiosondes were complemented by a large number of additional radiosondes during both the experiments.

Figure 3 – Picture of the experimental set-up during the Arctic Winter Radiometric Experiment 2004.

Results and discussion
AWRE 2004

The data collected by MWR, MWRP, and GSR during the AWRE were processed to give an experimental quantitative estimate of the sensitivity of cm-, mm- and submm-wave channels to changes in PWV and LWP. The calibrated Tbs were first divided into clear

and cloudy conditions according to the ARM operational LWP retrieval (based on MWR observations) and the sky infrared temperature measured by the 10 micron channel. Once clear-sky Tbs have been selected, the relationship with PWV is estimated by curve fitting. For each channel, the observed Tb was fitted with a line, resulting in the curves shown in Figure 4. The sensitivity of each channel to PWV variations is given by the slope of the fit (i.e., dTb/dPWV) at any value of PWV. Thus, channels with a relatively flat fit (as 22.235, 30, and 89 GHz) show little sensitivity to small PWV changes. These slopes remain nearly constant throughout the available range, indicating that these channels offer the same sensitivity regardless of the PWV absolute value. Similar considerations apply to 183.31±7 and 183.31±16 GHz channels, although here the sensitivity (i.e. slope) is larger.

Conversely, more opaque channels show non-linear relationship with PWV; the slope is very steep (i.e., high sensitivity) in a reduced range, but then the curve bends and the slope tends to zero (i.e., saturation). This is the case for 183.31±1 and 183.31±3 GHz channels, for which the sensitivity is not uniquely determined, but it is rather a function of PWV. Considering the slope values estimated from the data within the 0-1.5 mm PWV range, we found that the sensitivity of mm and submm channels to very low PWV outperforms the one at 20-30 GHz by a factor ranging from 1.5 to 69.

The next step is to quantify the channel sensitivity to LWP. Thus, we select cloudy-sky Tbs according to ARM operational LWP and MWRP Tir, and we remove the PWV contribution from Tb; this contribution is computed using the ARM operational PWV retrievals and the Tb-PWV relationship we have determined in the previous step. From Fig. 5 it is evident that 89 and 183.31±16 GHz channels present steeper slopes (i.e., larger sensitivity to LWP) with respect to 20-30 GHz, by a factor of 3 to 4. More details on the method and results are given in [Cimini et al., 2007b].

RHUBC 2007

More recently, the GSR, GVR, and MP-183A have been developed during RHUBC, offering the first opportunity to cross-check instrument performances and the quality of data taken during field experiments. In particular, the GSR, GVR, and MP-183A all have several channels located around the strong 183.31 GHz water vapor line. This fortunate situation gives us the opportunity to compare colocated independent observations and thus to evaluate the relative performances of the three instruments in the vicinity of the 183.31 GHz line. Although different design characteristics preclude direct comparison of Tb, these differences can be predicted indirectly in Tb space once the hardware characteristics are properly modeled. Figure 6 illustrates two examples of the comparison between independent measurements and the corresponding modeled predictions. Similar scatter plots were produced for all the independent channel pairs with similar spectral characteristics. For most of the comparisons the observed Tbs lie nicely over the simulations, which means that the systematic differences between the measurements are generally explained by the different hardware specification. Quantitatively, the experimental bias remains within 1.5 K from the simulation predictions, consistently with a ~1 K absolute accuracy for each instrument, while the standard deviation of the residuals remains within the expectations for a comparison of two independent variables with accuracy ~1-2 K.

Moreover, RHUBC provided the opportunity to evaluate the performances of the three instruments with respect to forward model simulations obtained from radiosoundings.
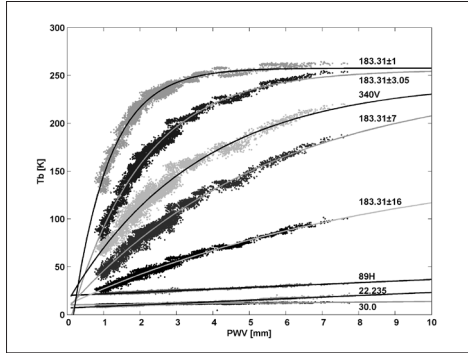
Figure 4 – Measured brightness temperature response to PWV in clear sky for selected MWRP and GSR channels. Lines through the observed data represent 2- and 3-parameter fit.
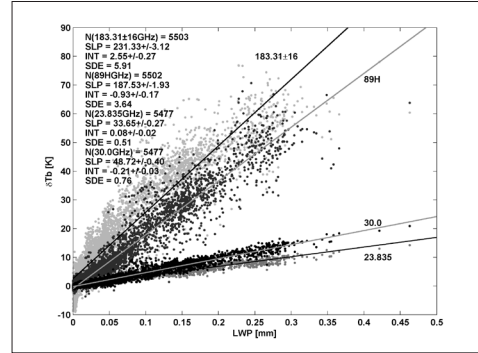
Figure 5 – Measured brightness temperature response to LWP for selected MWRP and GSR channels. Number of elements (N), slope (SLP) and intercept (INT) of a linear fit, standard estimation error (SDE) are reported. SLP is in K/mm, INT and SDE are in K. Uncertainties are the 99% confidence interval.

Simulations have been computed from the ARM radiosonde observations during clear sky (as detected by a colocated ceilometer) using version 3.3 of the MonoRTM code [Payne et al., 2008].

The radiometer measurements were averaged over a time period from 5 minutes before to 30 minutes after each radiosonde launch, to account for the time taken for the radiosonde to pas the tropopause. Figure 7 shows two example of this comparison. Overall, this analysis showed that the three instruments are consistent with forward model simulations within the expected accuracy. However, spectral features were found investigating Tb residuals, indicating some degree of inconsistency between the instruments and the forward model. The most likely cause of forward model error is systematic errors in the radiosonde humidity profiles used as input, as discussed in [Cimini et al., 2009]. In fact, in very dry conditions channels close to the line center are sensitive to upper troposphere-lower stratosphere humidity, which is not always accurately represented by radiosonde sensors.

Thus, results from AWRE and RHUBC demonstrated that (a) mm- and submm-wave channels have greatly improved sensitivity to low amounts of PWV and LWP and (b) the consistency between observed data generally confirms the specification accuracy. Combining these two considerations, it follows a high level of expected accuracy for PWV and LWP estimates.

Therefore, we developed a retrieval method for inverting GSR data into PWV and LWP estimates. The method used here is a simple a priori piece-wise linear statistical inversion, and used a 6-year database of radiosondings launched from NSA for the a priori ensemble.

The radiosounding database has been processed with a forward model to simulate Tbs at GSR channels and random Gaussian noise consistent with GSR specifications was added to the synthetic Tbs. Results for PWV retrievals are shown in Figure 8 for one day. The retrievals based on GSR observations are plotted together with the operational ARM PWV product (estimated from MWR) and PWV integrated from radiosounding profiles. Note the

excellent agreement between the GSR retrievals and the radiosondes and that the ARM MWR product has a bias of about 0.02 cm relative to the GSR and radiosondes. Also, evidently the retrievals from GSR are associated with a substantially reduced noise level with respect to MWR. This is due in part to the larger number of channels used in the retrieval (8 for GSR, 2 for MWR) and in part to the enhanced sensitivity of mm- and submm-wavelengths. A statistical comparison between both these PWV retrievals with respect to RAOB for the whole RHUBC experiment is in Figure 9. The GSR retrievals provided unprecedented accuracy in PWV retrievals of 0.1 mm rms with respect to RAOBs.
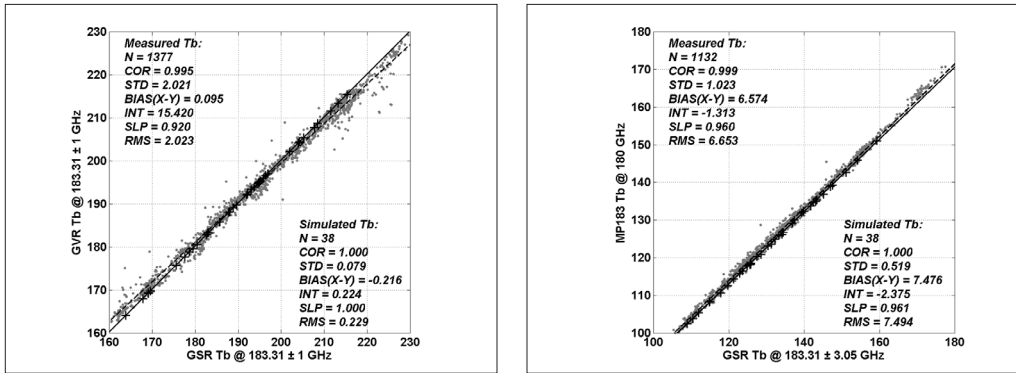

Figure 6 – Scatter plot of Tb from selected GVR and MP-183A channels vs GSR Tb at corresponding nearest channels (gray dots). Black crosses indicate the simulated Tb based on clear-sky RAOB. Lines show linear fit through observations (dashed) and simulations (continuous).
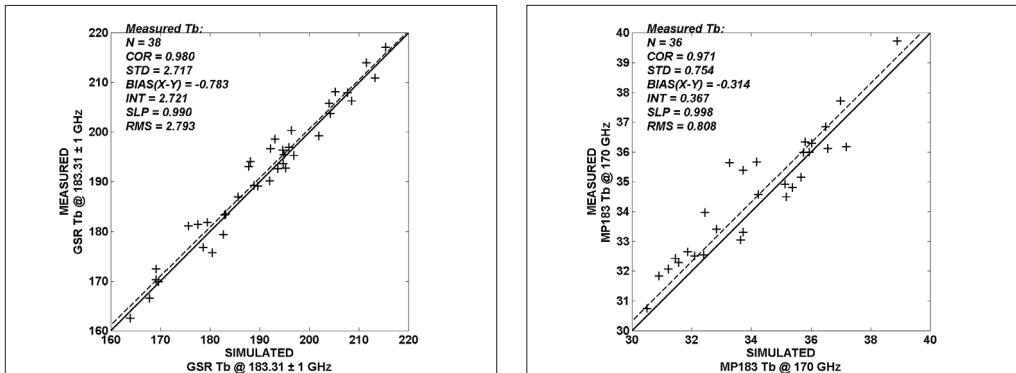

Figure 7 – Measured vs. simulated Tb from selected GSR and MP-183A channels. The black solid line represents the 1:1 line, while the dashed line shows the linear fit through the experimental data.

Conclusions

Ground-based observations at cm, mm, and submm wavelengths were collected during two field campaigns. Starting from both simulations and measurements outcomes, it was demonstrated that mm and submm wavelengths offer enhanced sensitivity with respect

to cm-wave radiometry to low amounts of PWV and LWP typical of the polar and high altitude regions. A quantitative study on the experimental data yields enhancement factors from 1.5 to 69 for PWV and 3 to 4 for LWP when compared to 22-31 GHz channels.
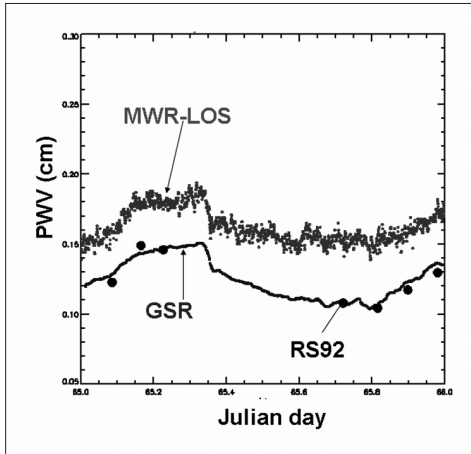

Figure 8 – Time series of PWV as retrieved from GSR, MWR, and measured by RS92 radiosoundings on March 6 2007 (Julian day 65).
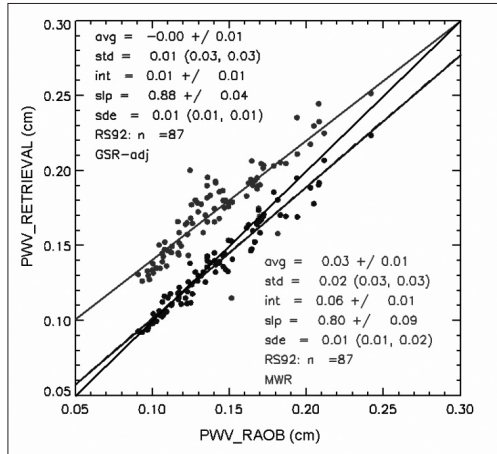
Figure 9 – Statistics of PWV retrieved from GSR and MWR with respect to RS92 radiosoundings measurements during RHUBC.

The instrument cross-comparison and the validation against RAOB-based simulations - taking into account the spectral characteristics - showed agreement generally within the total expected uncertainty (~1 K absolute accuracy, ~1-2 K rms accuracy). Due to the demonstrated enhanced sensitivity and instrument accuracy, mm- and submm-wavelength observations are expected to improve significantly the retrieval of PWV and LWP. Results obtained using a simple piece-wise linear statistical inversion showed an accuracy in PWV retrievals of 0.1 mm rms with respect to RAOBs. Finally, it is foreseen that the use of non-linear techniques would overcome the limitations imposed by the linear regression and exploit more fully the potential of GSR observations. Accordingly, a One Dimensional Variational Assimilation Retrieval (1D-VAR) is currently being implemented as part of our ongoing research.

Acknowledgements

References
Cimini D., Westwater E. R., Gasiewski A. J., Klein M., Leusky V., Dowlatshahi S. (2007a) - *The Ground-based Scanning Radiometer: A Powerful Tool for Study of the Arctic Atmosphere*.

IEEE TGRS, Vol. 45, No. 9, pp. 2759-2777.

Cimini D., Westwater E. R., Gasiewski A. J., Klein M., Leusky V., Liljegren J. (2007b) - *Ground-based millimeter- and submillimiter-wave observations of low vapor and liquid water contents*. IEEE TGRS, Vol. 45, No. 7, pp. 2169-2180.

Cimini D., Nasir F., Westwater E.R., Payne V. H., Turner D. D., Mlawer E. J., Exner M. L., Cadeddu M. (2009) - *Comparison of ground-based millimeter-wave observations in the Arctic winter*, IEEE TGRS, in press.

Mattioli V., Westwater E. R., Cimini D., Gasiewski A.J., Klein M., Leuski V.Y. (2008) - *Microwave and Millimeter-wave Radiometric and Radiosonde Observations in an Arctic Environment*. J. Atmos. Ocean. Technol., In press.

Payne V. H., Delamere J., Cady-Pereira K., Moncet J.L., Mlawer E., Clough T., Gamache R. (2008) - *Air-broadened half-widths of the 22 GHz and 183 GHz water vapor lines*. IEEE Trans. Geosci. Remote Sens., 46, 3601-3617.

Racette P. E., Westwater E. R., Han Y., Gasiewski A., Klein M., Cimini D., Manning W., Kim E., Wang J., Kiedron P. (2005) - *Measuring low amounts of precipitable water vapor using millimeter-wave radiometry*. J. Atmos. Ocean. Technol., Vol. 22, Vo. 4, pp. 317–337.

Shupe M. D., Uttal T., Matrosov S. (2005) - *Arctic Cloud Microphysics Retrievals from Surface-based Remote Sensors at SHEBA*. Journal of Applied Meteorology, Vol.44, 1544-1562.

Westwater E. R., Klein M., Leuski V., Gasiewski A. J., Uttal T., Hazen D. A., Cimini D., Mattioli V., Weber B. L., Dowlatshahi S., Shaw J. A., Liljegren J. S.,. Lesht B. M, Zak B. D. (2004) - *Initial Results from the 2004 North Slope of Alaska Arctic Winter Radiometric Experiment*. Proceedings. IGARSS, Anchorage, AK.